Journal of Dental Research
2015, Vol. 94(8) 1092–1098

DOI: 10.1177/0022034515589314
jdr.sagepub.com

Kinetic-dependent Killing of Oral Pathogens with Nitric Oxide

C.J. Backlund[1], B.V. Worley[1], A.R. Sergesketter[1], and M.H. Schoenfisch[1]

Abstract

Nitric oxide (NO)–releasing silica nanoparticles were synthesized via the co-condensation of tetramethyl orthosilicate with aminosilanes and subsequent conversion of secondary amines to *N*-diazeniumdiolate NO donors. A series of ~150 nm NO-releasing particles with different NO totals and release kinetics (i.e., half-lives) were achieved by altering both the identity and mol% composition of the aminosilane precursors. Independent of identical 2 h NO-release totals, enhanced antibacterial action was observed against the periodontopathogens *Aggregatibacter actinomycetemcomitans* and *Porphyromonas gingivalis* with extended NO-release kinetics at pH 7.4. Negligible bactericidal effect was observed against cariogenic *Streptococcus mutans* at pH 7.4, even when using NO-releasing silica particles with greater NO-release totals. However, antibacterial activity was observed against *S. mutans* at lower pH (6.4). This result was attributed to more rapid proton-initiated decomposition of the *N*-diazeniumdiolate NO donors and greater NO-release payloads. The data suggest a differential sensitivity to NO between cariogenic and periodontopathogenic bacteria with implications for the future development of NO-releasing oral care therapeutics.

Keywords: *N*-diazeniumdiolate, silica, dental caries, periodontal disease, *Aggregatibacter actinomycetemcomitans*, *Porphyromonas gingivalis*

Introduction

Silica particles are the key abrasive scouring agents in toothpastes that facilitate the removal of bacteria (Barbe et al. 2004; Brunner et al. 2006; Riccio and Schoenfisch 2012). Recent evidence suggests that polishing with nanoparticles versus micron-sized silica helps decrease the surface roughness of teeth and further lessens the strength of bacterial adhesion, making *Streptococcus mutans* removal easier (Gaikwad and Sokolov 2008). Although effective at reducing overall bacterial counts, silica nanoparticles are not inherently antimicrobial. Various materials, including fibers, gels, polymers, and microspheres, modified to release antibiotics (e.g., minocycline), have demonstrated promise for the treatment of oral diseases (Greenstein and Polson 1998; Williams et al. 2001). Unfortunately, these materials are less suitable for the physical removal of plaque-forming bacteria. While local drug delivery systems may limit the risk of systemic side effects (e.g., pseudomembranous colitis) (Radvar et al. 1996; Williams et al. 2001), the overuse of antibiotics fosters antibiotic-resistant pathogens (Kinane and Radvar 1999). The combination of silica (as a polishing agent) with new antibacterial agents that do not foster bacterial resistance could potentially lead to improved therapeutics for treating periodontal disease and dental caries that are easily implemented into existing dental hygiene practices (i.e., teeth brushing).

Nitric oxide (NO) is a gaseous free radical produced endogenously during the immune response to invading organisms (Bogdan 2001). In oral biology, both bacteria and proinflammatory stimuli present in dental plaque biofilms elicit the generation of NO from oral mucosal epithelial cells (Carossa et al. 2001). The antibacterial activity of NO is attributed to reactive by-products causing oxidative and nitrosative stresses on bacteria. For example, NO reacts with superoxide to form peroxynitrite, which elicits significant membrane damage via lipid peroxidation, while reaction with oxygen produces dinitrogen trioxide, a nitrosative species that disables protein function (Hetrick and Schoenfisch 2006). With broad-spectrum activity and no observed bacterial resistance to date (Privett et al. 2012; Schairer et al. 2012), the delivery of exogenous NO is a promising antibacterial for oral care. Although NO produced via the acidification of nitrite has bactericidal properties against cariogenic (Silva Mendez et al. 1999) and periodontopathogenic bacteria (Allaker et al. 2001), precise control over NO generation is pivotal in designing effective antibacterial delivery systems (Barbe et al. 2004; Carpenter and Schoenfisch 2012).

[1]Department of Chemistry, University of North Carolina at Chapel Hill, Chapel Hill, NC, USA

A supplemental appendix to this article is published electronically only at http://jdr.sagepub.com/supplemental.

Corresponding Author:
M.H. Schoenfisch, Department of Chemistry, University of North Carolina at Chapel Hill, Chapel Hill, NC 27599-3290, USA.
Email: schoenfisch@unc.edu

Shin et al. (2007) first reported the Stöber (Stöber et al. 1968) synthesis of hybrid NO-releasing silica nanoparticles of varying size (20–500 nm). The aminosilane composition (10–87 mol%) of the silica nanoparticles was tunable, which enabled a thorough evaluation of NO's utility against Gram-positive, Gram-negative, and fungal biofilms (Shin et al. 2007; Hetrick et al. 2009). Subsequent research has focused on studying the physicochemical properties (e.g., size, shape, and release kinetics) of NO donor-modified silica nanoparticles to maximize bactericidal efficacy. Carpenter et al. (2011) observed that ~50 nm NO-releasing silica particles were more effective at killing bacteria than larger particles (e.g., 100 and 200 nm) due to enhanced diffusion and faster bacteria-particle association. Lu et al. (2013) described the synthesis of NO-releasing silica rods, noting improved bactericidal activity for oblong over spherical particles due to increased bacteria/particle surface contact and intracellular NO delivery. In the same study, a greater initial NO flux showed improved killing, suggesting that faster NO-release kinetics may enhance NO's antibacterial activity against *Pseudomonas aeruginosa* (Lu et al. 2013). To date, the antibacterial activity of NO-releasing silica nanoparticles as a function of NO-release kinetics has not been systematically evaluated, particularly against oral pathogens.

Herein, we investigated the influence of NO-release kinetics on bactericidal efficacy against common periodontopathogens independent of particle size and NO-release totals. Comparatively, the kinetic-dependent killing of a cariogenic strain was also examined using a single NO-releasing silica particle system with greater NO-release totals.

Materials and Methods

Materials

Materials are described in the Appendix.

Synthesis of NO-releasing Silica Particles

The Stöber co-condensation of aminosilanes with alkoxysilanes was used to create secondary amine-modified silica particles. Briefly, hybrid particles were synthesized by combining tetramethyl orthosilicate (TMOS) with an aminosilane (3-methylaminopropyltrimethoxysilane [MAP3], *N*-(6-aminohexyl) aminopropyltrimethoxysilane [AHAP3], and *N*-(2-aminoethyl)-3-aminopropyltrimethoxysilane [AEAP3]) and injection of the silane mixture into a flask containing water, ammonium hydroxide, and EtOH; stirring for 2 h under ambient conditions; and collecting via centrifugation. Secondary amines were converted to *N*-diazeniumdiolate NO donors under high pressures of NO gas in basic conditions. The control and NO-releasing silica particles were characterized using dynamic light scattering, scanning electron microscopy, carbon, hydrogen, and nitrogen (CHN) elemental analysis, and chemiluminescent nitric oxide detection. Complete synthesis and characterization of NO-releasing hybrid silica nanoparticles are described in the Appendix.

Bactericidal Assays

Complete bacterial growth is described in the Appendix. Briefly, *Streptococcus mutans, Aggregatibacter actinomycetemcomitans*, and *Porphyromonas gingivalis* were grown to 10^8 colony-forming units (CFU)/mL, pelleted via centrifugation, and diluted to 10^6 CFU/mL. Bacteria solutions were added to vials containing either NO-releasing or control silica, sonicated, and incubated aerobically at 37 °C with moderate shaking. After 2 h, these solutions were diluted and spiral-plated using an Eddy Jet spiral plater (IUL, Farmingdale, NY, USA) on BHI agar or Wilkins-Chalgren agar (*P. gingivalis*) and incubated at 37 °C under aerobic (*S. mutans*, 3 d), microaerophilic (*A. actinomycetemcomitans*, 2 d), or anaerobic (*P. gingivalis*, 4 d) conditions. Viable colonies were enumerated on agar plates using a Flash and Go colony counter (IUL). The concentration resulting in a 3-log reduction in bacterial viability to below 2.5×10^3 CFU/mL (limit of detection for the plating method) (Breed and Dotterrer 1916) was determined to be the minimal bactericidal concentration (MBC_{2h}).

Confocal Microscopy for Intracellular NO Detection

Confocal microscopy assays for the detection of intracellular NO in planktonic cultures of *A. actinomycetemcomitans* and *S. mutans* are described in the Appendix.

In Vitro Cytotoxicity

Human gingival fibroblasts (HGF-1) were grown in Dulbecco's modified Eagle's medium (DMEM) supplemented with 10% (v/v) fetal bovine serum (FBS) and 1 wt% penicillin streptomycin (PS) and incubated at 37 °C under humidified conditions in 5% CO_2 (v/v). At 80% confluency, cells were trypsinized, seeded onto a tissue culture–treated 96-well plate, and incubated at 37 °C. Solutions of control and NO-releasing silica particles (8, 32, and 48 mg/mL for 80 mol% AEAP3, 60 mol% AHAP3, and 50 mol% MAP3, respectively) in DMEM were added to the cells before a 2 h incubation at 37 °C. The supernatant was then aspirated, and 120 µL DMEM/phenazine methosulfate (PMS)/3-(4,5-dimethylthiazol-2-yl)-5-(3-carboxymethoxyphenyl)-2-(4-sulfophenyl)-2H-tetrazolium inner salt (MTS) solution (100/20/1 v/v/v) was added to the wells. After a 2 h incubation at 37 °C, 100 µL from each well was transferred to a new microtiter plate. A Multiskan EX plate reader (Thermo Scientific, Waltham, MA, USA) was used to measure the absorbance at 490 nm. The absorbance measurements were blank-subtracted, and cell viability was quantified relative to untreated cells.

Results

Hybrid alkoxysilane/aminosilane silica nanoparticles were synthesized via the Stöber method (Stöber et al. 1968). Through careful variation of the synthetic reaction parameters, MAP3, AHAP3, and AEAP3 silica nanoparticles were produced to

Table. Characterization of NO-Releasing Silica Particles in Phosphate-Buffered Saline (pH 6.4 or 7.4, 37 °C) as Measured by a Chemiluminescence NO Analyzer.

NO Release Scaffold	pH	t[NO] (μmol/mg)[a]	$[NO]_m$ (ppb/mg)[b]	$t_{½}$ (min)[c]	$t[NO]_{2h}$ (μmol/mg)[d]
50% MAP3	7.4	0.22 ± 0.04	900 ± 300	31.6 ± 6.7	0.19 ± 0.04
60 % AHAP3	7.4	0.25 ± 0.05	1,700 ± 1,000	33.8 ± 5.5	0.21 ± 0.04
80% AEAP3	7.4	0.39 ± 0.05	1,400 ± 200	112.5 ± 18.0	0.20 ± 0.02
70% MAP3	7.4	0.84 ± 0.14	9,200 ± 4,300	19.8 ± 3.3	0.81 ± 0.15
70% MAP3	6.4	0.95 ± 0.17	25,800 ± 7,500	4.5 ± 0.2	0.95 ± 0.17

Results shown for 50 mol% MAP3, 60 mol% AHAP3, 80 mol% AEAP3, and 70 mol% MAP3 NO-releasing silica particles and presented as mean ± standard deviation for $n = 3$ or more pooled experiments. AEAP3, *N*-(2-aminoethyl)-3-aminopropyltrimethoxysilane; AHAP3, *N*-(6-aminohexyl) aminopropyltrimethoxysilane; MAP3, 3-methylaminopropyltrimethoxysilane; NO, nitric oxide.
[a]Total NO released.
[b]Maximum NO flux.
[c]NO-release half-life.
[d]Total NO released after 2 h.

have similar geometric diameters (~150 nm) and a high degree of monodispersity, as indicated by the low polydispersity index (PDI) values (≤0.06; Appendix). Successful incorporation of the aminosilanes was confirmed via CHN elemental analysis with an increase in nanoparticle nitrogen wt% (3.42, 4.28, and 5.83 wt% for MAP3, AHAP3, and AEAP3, respectively; Appendix). The positively charged (i.e., protonated) surface amines of the particles resulted in positive zeta potentials (Appendix). In Tris–phosphate-buffered saline (PBS) (pH 7.4), MAP3 and AEAP3 particles were characterized as having similar zeta potentials (~20 mV), while AHAP3 particles exhibited a greater positive surface charge (31.4 mV).

NO release from MAP3, AHAP3, and AEAP3 particles was characterized using chemiluminescence in PBS (pH 7.4) at 37 °C to obtain NO-release totals and kinetics (i.e., half-lives) (Coneski and Schoenfisch 2012). The total NO release for the MAP3, AHAP3, and AEAP3 particles was 0.22, 0.25, and 0.39 μmol/mg, respectively (Table). Of importance, the 2 h NO-release totals were similar (~0.20 μmol/mg) across all 3 particle systems and representative of the NO concentration delivered during the 2 h bacteria killing assays. The NO-release half-lives were also similar for MAP3 and AHAP3 (~32 min) but significantly longer for AEAP3 (112.5 min).

To study the role of NO-release kinetics and particle surface charge on bactericidal efficacy, 2 h bacteria killing assays were conducted against periodontopathogens in Tris-PBS (pH 7.4; 37 °C). Lower bactericidal concentrations (MBC_{2h}) were observed for AHAP3 over MAP3 particles against both *A. actinomycetemcomitans* (32 vs. 48 mg/mL, respectively) and *P. gingivalis* (16 vs. 32 mg/mL, respectively) (Figure 1). The bactericidal concentrations for NO-releasing AEAP3 were 8 mg/mL against both periodontopathogens, corresponding to a bactericidal NO dose of 1.6 μmol/mL. This NO dose is reduced from that of NO-releasing MAP3 (9.1 and 6.1 μmol/mL against *A. actinomycetemcomitans* and *P. gingivalis*, respectively). Human gingival fibroblasts (HGF-1) were used to evaluate the toxicity of NO-releasing and control silica particles at bactericidal concentrations. The toxicity of control particles increased (i.e., decreased cell viability) as a function of the silica concentration (Figure 2). For the AHAP3 and MAP3 particle systems, NO release further decreased cell viability (31% and 21% relative to untreated cells). The addition of NO release for the AEAP3 system, however, improved HGF-1 viability to relatively nontoxic levels (>80% viability).

Due to the decreased sensitivity of the cariogenic pathogen *S. mutans* to NO (Backlund et al. 2014), the NO storage for the most rapid NO-releasing system (MAP3) was increased to ~1 μmol/mg. Bactericidal assays were performed at both pH 7.4 and 6.4 to evaluate the effects of faster NO-release kinetics on biocidal action. At pH 6.4, MAP3 NO-release kinetics were more rapid as *N*-diazeniumdiolate donors decompose faster with increasing proton concentration, resulting in a greater initial NO flux (9,200 to 25,800 ppb/mg) and shorter half-life (19.8 to 4.5 min) (Table). The zeta potential for MAP3 particles at pH 6.4 (26.3 mV) also indicated a greater positive charge, due to greater amine protonation at lower pH. While increasing the total NO payload at pH 7.4 did not enhance *S. mutans* killing by NO-releasing MAP3 particles, complete eradication of *S. mutans* (i.e., 3-log reduction in viability) at pH 6.4 was achieved with 32 mg/mL MAP3 particles (Appendix).

Discussion

In this study, we synthesized NO-releasing silica nanoparticles of varying aminosilane identity and composition (50 mol% MAP3, 60 mol% AHAP3, and 80 mol% AEAP3) to investigate the role of NO-release kinetics on the killing of periodontal pathogens. For clarity, the particle systems are referred to as MAP3, AHAP3, and AEAP3. Synthetic parameters were tuned to produce monodisperse nanoparticles with similar geometries and diameters. Maintaining a constant size was crucial as this parameter has been shown to influence bactericidal efficacy (Carpenter et al. 2011). Incorporating different aminosilanes into the nanoparticles allowed us to investigate the effects of particle surface charge on bactericidal action, with AHAP3 particles exhibiting a greater positive surface charge than either MAP3 or AEAP3. Furthermore, as the kinetics of proton-initiated *N*-diazeniumdiolate decomposition from NO donors are dependent on structure (Shin et al. 2007), NO-release kinetics

were varied with aminosilane identity as well. The significantly longer NO-release half-life observed for AEAP3 over MAP3 or AHAP3 particles is due to *N*-diazeniumdiolate stabilization via hydrogen bonding with neighboring cationic amines on the AEAP3 scaffold (Lu et al. 2011). The ability to tune both the identity and degree of silica nanoparticle aminosilane functionalization while maintaining constant geometric diameters decoupled particle size–mediated killing from NO release and particle surface charge. The bactericidal efficacy of MAP3 and AEAP3 was thus compared as a function of NO-release kinetics, independent of particle size, surface charge, and 2 h NO-release totals. The influence of particle surface charge was compared between MAP3 and AHAP3 particles, independent of NO-release kinetics. Last, we evaluated the importance of increased positive particle surface charge (AHAP3) versus extended NO-release kinetics (AEAP3) on periodontopathogen killing.

As expected from our previous work (Backlund et al. 2014), both *A. actinomycetemcomitans* and *P. gingivalis* were readily susceptible to NO, with bactericidal NO doses of <10 µmol/mL (Fig. 1). However, bactericidal efficacy was also dependent on both NO-release kinetics and particle surface charge. Increased bactericidal action was observed for AHAP3 over MAP3 particles against both periodontopathogens. Due to the similar NO-release half-lives (~32 min) of these systems, the improved bactericidal efficacy of AHAP3 was attributed to the increased particle surface charge (31.4 vs. 20.9 mV for AHAP3 and MAP3, respectively). Greater positive surface charge enhances particle-bacteria association (Aoki et al. 2012) and most likely increases the buildup of intracellular NO and thus NO-mediated death. Confocal microscopy and the fluorescent probe DAF-2 DA confirmed greater NO delivery to *A. actinomycetemcomitans* from AHAP3 versus MAP3 particles over a 30 to 120 min window (Fig. 3). In contrast, intracellular NO from the MAP3 particle system was observed only after 120 min. The improved antibacterial activity of NO-releasing AHAP3 over MAP3 particles is thus attributed to the more efficient delivery of NO with increasing surface charge.

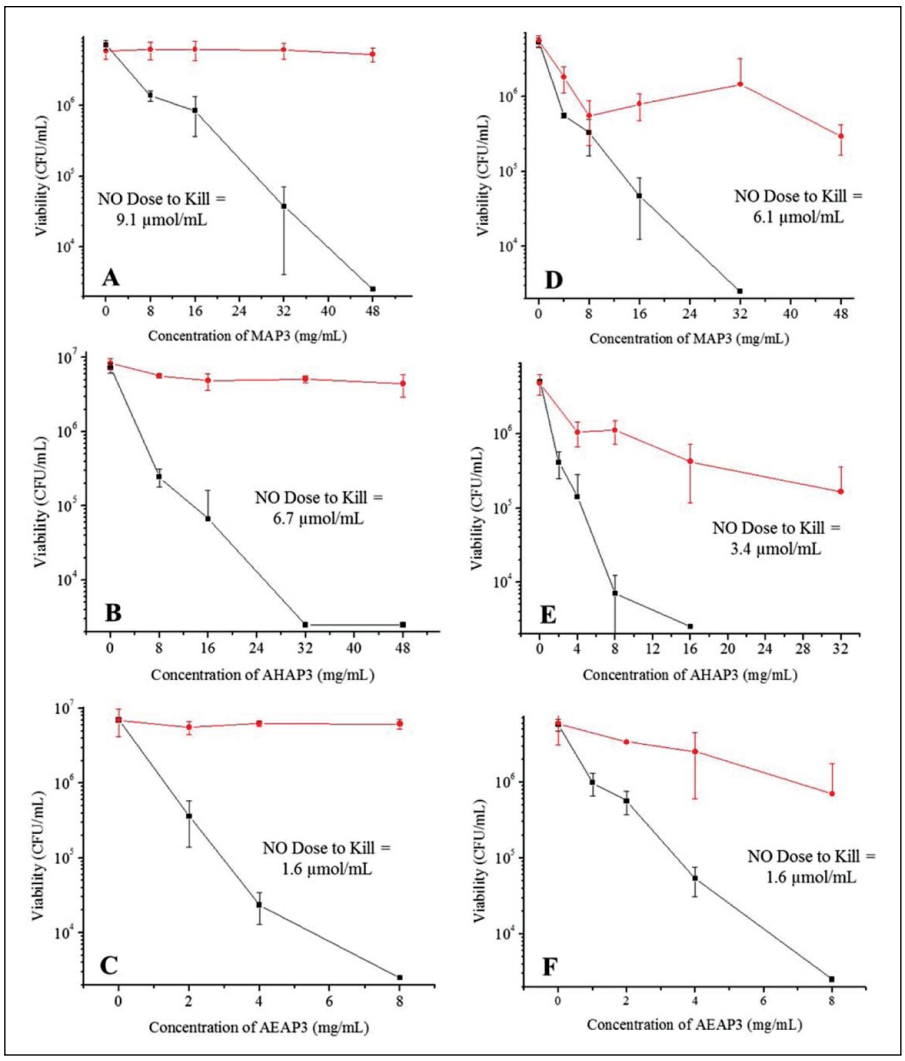

Figure 1. Bactericidal efficacy of (**A**) 50 mol% 3-methylaminopropyltrimethoxysilane (MAP3) particles, (**B**) 60 mol% *N*-(6-aminohexyl)aminopropyltrimethoxysilane (AHAP3) particles, and (**C**) 80 mol% *N*-(2-aminoethyl)-3-aminopropyltrimethoxysilane (AEAP3) particles against *Aggregatibacter actinomycetemcomitans* in Tris–phosphate-buffered saline (PBS) (pH 7.4) after 2 h. Bactericidal efficacy of (**D**) 50 mol% MAP3 particles, (**E**) 60 mol% AHAP3 particles, and (**F**) 80 mol% AEAP3 particles against *Porphyromonas gingivalis* in Tris-PBS (pH 7.4) after 2 h. Nitric oxide (NO)–releasing material denoted by rectangles (■) and non-NO-releasing controls denoted by circles (●). Error bars signify standard deviation of the mean bacterial viability (colony-forming units [CFU]/mL). For all measurements, $n = 3$ or more pooled experiments.

The most effective killing of periodontopathogens was observed for NO-releasing AEAP3 particles (Fig. 1). We hypothesized that the extended NO-release kinetics (i.e., half-lives) characteristic of AEAP3 (112.5 min) compared with MAP3 (31.6 min) particles facilitated the enhanced killing. Intracellular NO fluorescence was observed for the AEAP3 particle system after only 30 min of exposure to *A. actinomycetemcomitans* compared with MAP3, which required 120 min for any visible fluorescence (Fig. 3). Furthermore, the intracellular NO from AEAP3 increased to a maximum at 60 min before decreasing at 120 min, coinciding with outer membrane decomposition and bacterial death (Hetrick et al. 2008; Slomberg et al. 2013).

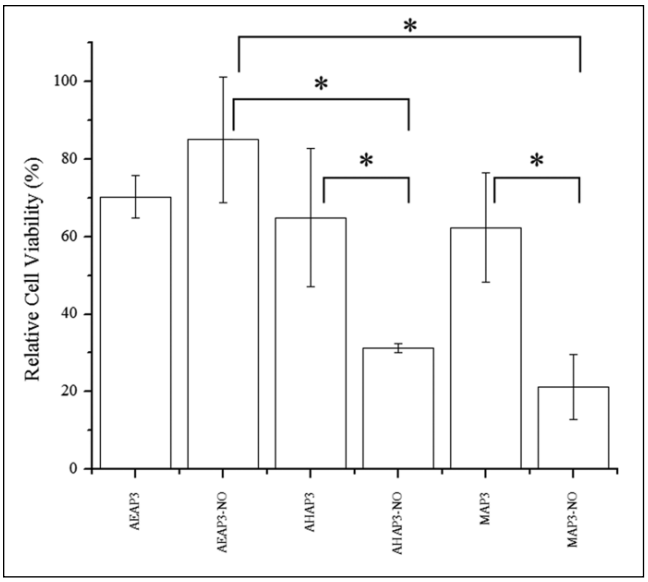

Figure 2. Cytotoxicity of nitric oxide (NO)–releasing and control silica particles against HGF-1 human gingival fibroblasts at the greatest MBC_{2h} values to kill periodontopathogens. The concentrations to kill *Aggregatibacter actinomycetemcomitans* were 8, 32, and 48 mg/mL for 80 mol% *N*-(2-aminoethyl)-3-aminopropyltrimethoxysilane (AEAP3), 60 mol% *N*-(6-aminohexyl)aminopropyltrimethoxysilane (AHAP3), and 50 mol% 3-methylaminopropyltrimethoxysilane (MAP3), respectively. Viability measured as metabolic activity versus untreated cells. Error bars represent standard deviation of the mean. For all values, $n = 4$ replicate measurements. Asterisk indicates $P < 0.05$ using 2-tailed Student's *t* test.

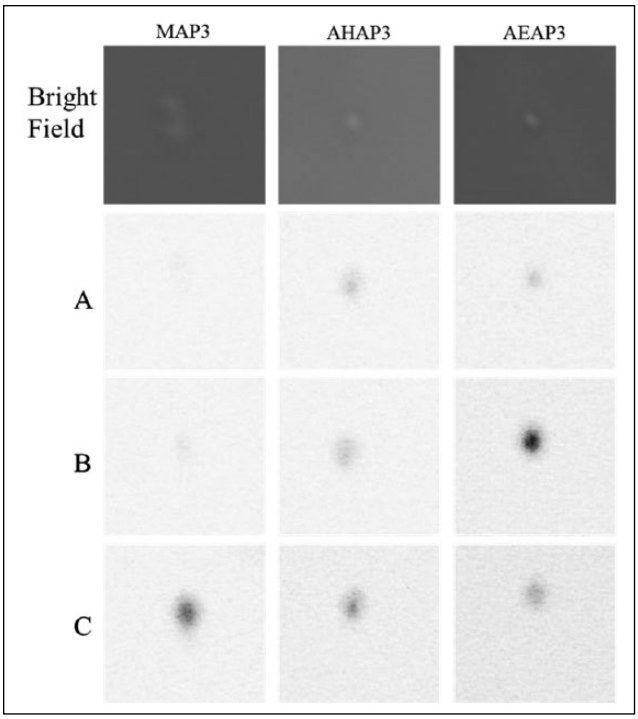

Figure 3. Confocal microscopy images of *Aggregatibacter actinomycetemcomitans* exposed to 1 mg/mL nitric oxide (NO)–releasing silica nanoparticles (50 mol% 3-methylaminopropyltrimethoxysilane [MAP3], 60 mol% *N*-(6-aminohexyl)aminopropyltrimethoxysilane [AHAP3], and 80 mol% *N*-(2-aminoethyl)-3-aminopropyltrimethoxysilane [AEAP3]) after (**A**) 30 min, (**B**) 60 min, and (**C**) 120 min of particle exposure. DAF-2 fluorescence is depicted as black in this image for clarity and represents intracellular NO concentrations.

The antibacterial activity of NO-releasing AHAP3 and AEAP3 particles was compared to evaluate the relative importance of increased positive particle surface charge versus extended NO-release kinetics for enhancing the bactericidal efficacy of NO-releasing silica particles. Despite the decreased particle surface charge for AEAP3 versus AHAP3 particles, NO-releasing AEAP3 exhibited greater antibacterial action. The increased bactericidal activity of NO-releasing AEAP3 suggests that extended NO-release kinetics may be more beneficial for killing periodontopathogens than a greater positive particle surface charge and enhanced particle-bacteria association. Confocal microscopy confirmed more efficient NO delivery to *A. actinomycetemcomitans* from NO-releasing AEAP3 versus AHAP3 particles (Fig. 3). While intracellular NO was detected for both NO-releasing particle systems after 30 min, the greater fluorescence signal observed for NO-releasing AEAP3 particles at 60 min indicates more accumulation of intracellular NO from AEAP3 versus AHAP3 particles. As such, NO-releasing AEAP3 particles more efficiently deliver bactericidal levels of NO within 120 min, resulting in cell death (Hetrick et al. 2008; Slomberg et al. 2013). The visualization of intracellular NO concentrations confirms the benefit of slower NO-release kinetics over greater (positive) particle surface charge for enhancing the bactericidal action of NO-releasing macromolecular scaffolds against periodontopathogens.

The improvement in the antibacterial activity of NO-releasing silica against periodontopathogens with extended NO-release kinetics was somewhat surprising as it contradicts previous reports. For example, Lu et al. (2013) observed that a greater initial NO flux and more rapid NO-release kinetics enhanced the bactericidal efficacy of silica-based NO release against *P. aeruginosa*. Of importance, *P. aeruginosa* uses the enzyme nitric oxide reductase (NOR) as a defense against NO-based host immunity (Kakishima et al. 2007), which functions as an NO detoxification mechanism by mitigating low concentrations of intracellular NO. Under such conditions, larger instantaneous NO concentrations are required to overload protective processes and elicit NO-mediated death. Conversely, *A. actinomycetemcomitans* and *P. gingivalis* do not possess these antioxidative pathways and are unable to effectively eliminate intracellular NO. Rather, as NO accumulates within the bacteria over time, NO-releasing silica particles that can associate with bacteria prior to releasing a majority of their NO payload (slow NO-releasing AEAP3 particles) more effectively deliver bactericidal levels of NO than fast NO-releasing systems that may release substantial amounts of NO prior to association with bacteria. The instantaneous NO concentration appears to be less critical for killing periodontal pathogens than total intracellular NO delivered over time. The benefit of extended NO-release kinetics for more effective periodontopathogen killing may influence the design of NO-releasing therapeutics for periodontal

diseases treatments. The combination of extended NO-release kinetics and greater positive surface charge might further enhance bactericidal efficacy.

The cytotoxicity of NO-releasing and control silica particles was evaluated against HGF-1 cells at bactericidal concentrations. While the addition of NO release increased the toxicity of MAP3 and AHAP3 particles, it was found to slightly decrease the cytotoxicity of AEAP3 particles. While NO-releasing AEAP3 particles demonstrated a general decrease in toxicity compared with the other NO-releasing systems, the increase in cell viability was not statistically significant from non-NO-releasing particles. The ability of HGF-1 cells to tolerate low instantaneous levels of intracellular NO, such as those provided by AEAP3, is attributed to the enzymatic breakdown of superoxide (O_2^-) by superoxide dismutase, an enzyme that limits the formation of reactive NO by-products and concomitantly mitigates the nitrosative and oxidative stresses associated with NO-mediated killing (Fridovich 1983). The increase in cell viability is likely the result of NO stimulating cell growth as reported previously (Papapetropoulos et al. 1997; Carpenter et al. 2012; Worley et al. 2014). The antibacterial characteristics and low cytotoxicity of the NO-releasing AEAP3 system warrant further investigation into slow NO-releasing silica-based materials as periodontal therapeutics. Increasing the total NO payload while maintaining slow-release kinetics may prove optimal in the clinical implementation of NO-based oral therapeutics.

We previously reported reduced sensitivity of *S. mutans* to NO treatment compared with periodontopathogens (Backlund et al. 2014). *S. mutans* is a unique pathogen that generates NO from nitrite via nitrite reductase to protect itself in nitrite-rich acidic environments such as the mouth (Choudhury et al. 2007; Backlund et al. 2014). Clearly, *S. mutans* possesses a mechanism to mitigate intracellular NO, thus limiting the antibacterial activity of both NO and its reactive by-products. As larger levels of NO are required to eradicate this cariogenic bacteria, particles with greater total NO storage were employed. However, the NO-releasing 70% MAP3 particles were incapable of eradicating *S. mutans* at pH 7.4. We hypothesized that faster NO release might overload this protective mechanism and facilitate *S. mutans* killing. To accelerate the NO-release kinetics of MAP3, NO-release characterization and bacterial killing assays were conducted at lower pH (6.4) in addition to physiological pH 7.4. Indeed, at pH 6.4, NO-releasing MAP3 particles resulted in total *S. mutans* killing at 32 mg/mL. This was attributed to the combination of faster NO release and positive surface charge at lower pH, leading to more efficient delivery of bactericidal levels of NO. Indeed, confocal microscopy confirmed more efficient NO delivery at pH 6.4 over pH 7.4, with greater intracellular NO levels detectable after 60 min (Fig. 4). Of note, the susceptibility of cariogenic bacteria to rapid NO release under acidic conditions may represent a viable method for the treatment of dental caries on short time scales (i.e., tooth brushing).

Conclusively, our study details the synthesis of ~150-nm NO-releasing silica nanoparticles with tunable NO-release kinetics and their antibacterial activity. Slower NO-release kinetics enhanced the bactericidal efficacy of NO-releasing silica particles against periodontopathogens while only minimally affecting human gingival fibroblast viability. The enhanced antibacterial action and reduced cytotoxicity for macromolecular NO-release scaffold that slowly releases NO warrant careful attention with respect to the development of NO-releasing therapeutics against periodontopathogens. A differential sensitivity to NO-release totals and kinetics was observed between periodontopathogens and cariogenic bacteria. The incorporation of additional biocides onto NO-releasing silica nanoparticles would be required to facilitate more complete killing of *S. mutans*.

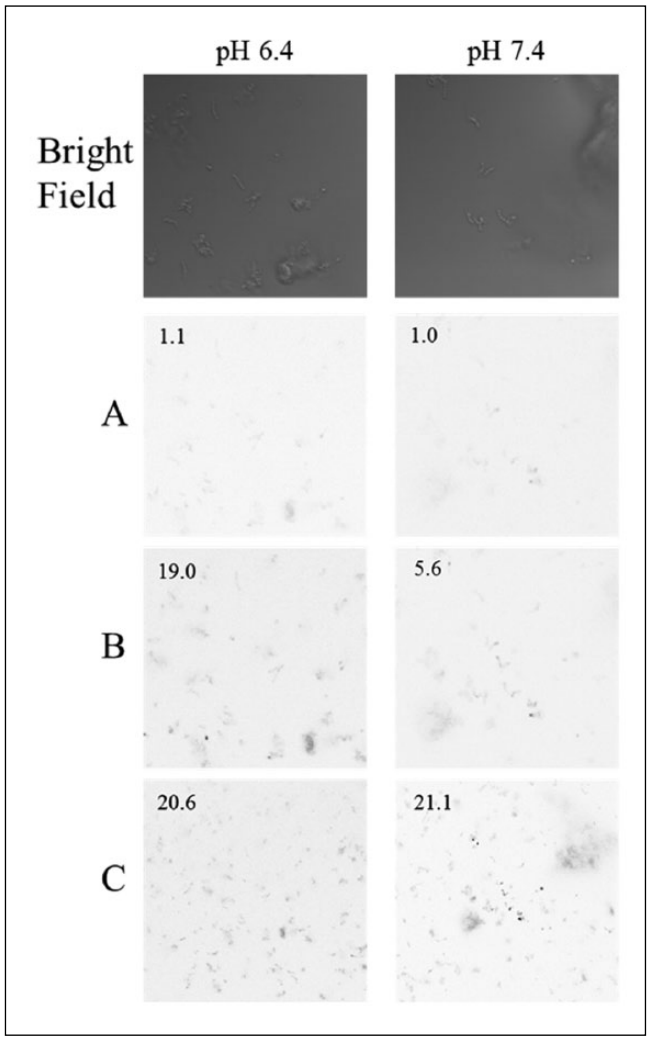

Figure 4. Confocal microscopy images of *Streptococcus mutans* exposed to 0.25 mg/mL 70 mol% 3-methylaminopropyltrimethoxysilane (MAP3) nitric oxide–releasing silica nanoparticles at (**A**) 40 min, (**B**) 60 min, and (**C**) 90 min after particle exposure. DAF-2 fluorescence is depicted as black in the images for clarity. Numbers in images represent the relative summed signal intensities normalized to the fluorescence intensity at 0 min and pH 7.4.

Author Contributions

C.J. Backlund, B.V. Worley, contributed to conception, design, data acquisition, analysis, and interpretation, drafted and critically

revised the manuscript; A.R. Sergesketter, contributed to conception, design, and data analysis, drafted and critically revised the manuscript; M.H. Schoenfisch, contributed to conception, design, data analysis, and interpretation, drafted and critically revised the manuscript. All authors gave final approval and agree to be accountable for all aspects of the work.

Acknowledgments

This research was supported by the National Science Foundation (DMR 1104892) and the National Institutes of Health (DE025207). The authors thank Michael Chua of the Michael Hooker Microscopy Facility at the University of Carolina at Chapel Hill for confocal microscopy assistance and Ning Yu of the UNC Dental School for providing *Porphyromonas gingivalis* (strain A7436). The corresponding author declares a competing financial interest. Mark Schoenfisch is a co-founder, is a member of the board of directors, and maintains a financial interest in Novan Therapeutics, Inc. Novan is commercializing macromolecular nitric oxide storage and release vehicles for dermatological indications. The authors declare no further potential conflicts of interest with respect to the authorship and/or publication of this article.

References

Allaker R, Silva Mendez L, Hardie J, Benjamin N. 2001. Antimicrobial effect of acidified nitrite on periodontal bacteria. Oral Microbiol Immunol. 16(4):253–256.

Aoki W, Kuroda K, Ueda M. 2012. Next generation of antimicrobial peptides as molecular targeted medicines. J Biosci Bioeng. 114(4):365–370.

Backlund CJ, Sergesketter AR, Offenbacher S, Schoenfisch MH. 2014. Antibacterial efficacy of exogenous nitric oxide on periodontal pathogens. J Dent Res. 93(11):1089–1094.

Barbe C, Bartlett J, Kong L, Finnie K, Lin HQ, Larkin M, Calleja S, Bush A, Calleja G. 2004. Silica particles: a novel drug-delivery system. Adv Mater. 16(21):1959–1966.

Bogdan C. 2001. Nitric oxide and the immune response. Nat Immunol. 2(10):907–916.

Breed RS, Dotterrer W. 1916. The number of colonies allowable on satisfactory agar plates. J Bacteriol. 1(3):321–331.

Brunner TJ, Wick P, Manser P, Spohn P, Grass RN, Limbach LK, Bruinink A, Stark WJ. 2006. In vitro cytotoxicity of oxide nanoparticles: comparison to asbestos, silica, and the effect of particle solubility. Environ Sci Tech. 40(14):4374–4381.

Carossa S, Pera P, Doglio P, Lombardo S, Colagrande P, Brussino L, Rolla G, Bucca C. 2001. Oral nitric oxide during plaque deposition. Eur J Clin Invest. 31(10):876–879.

Carpenter AW, Schoenfisch MH. 2012. Nitric oxide release, part II: therapeutic applications. Chem Soc Rev. 41(10):3742–3752.

Carpenter AW, Slomberg DL, Rao KS, Schoenfisch MH. 2011. Influence of scaffold size on bactericidal activity of nitric oxide–releasing silica nanoparticles. ACS Nano. 5(9):7235–7244.

Carpenter AW, Worley BV, Slomberg DL, Schoenfisch MH. 2012. Dual action antimicrobials: nitric oxide release from quaternary ammonium-functionalized silica nanoparticles. Biomacromolecules. 13(10):3334–3342.

Choudhury T, Sato E, Inoue M. 2007. Nitrite reductase in *Streptococcus mutans* plays a critical role in the survival of this pathogen in oral cavity. Oral Microbiol Immunol. 22(6):384–389.

Coneski PN, Schoenfisch MH. 2012. Nitric oxide release, part III: measurement and reporting. Chem Soc Rev. 41(10):3753–3758.

Fridovich I. 1983. Superoxide radical: an endogenous toxicant. Ann Rev Pharmacol Toxicol. 23:239–257.

Gaikwad R, Sokolov I. 2008. Silica nanoparticles to polish tooth surfaces for caries prevention. J Dent Res. 87(10):980–983.

Greenstein G, Polson A. 1998. The role of local drug delivery in the management of periodontal diseases: a comprehensive review. J Periodontol. 69(5):507–520.

Hetrick EM, Schoenfisch MH. 2006. Reducing implant-related infections: active release strategies. Chem Soc Rev. 35(9):780–789.

Hetrick EM, Shin JH, Paul HS, Schoenfisch MH. 2009. Anti-biofilm efficacy of nitric oxide–releasing silica nanoparticles. Biomaterials. 30(14):2782–2789.

Hetrick EM, Shin JH, Stasko NA, Johnson CB, Wespe DA, Holmuhamedov E, Schoenfisch MH. 2008. Bactericidal efficacy of nitric oxide–releasing silica nanoparticles. ACS Nano. 2(2):235–246.

Kakishima K, Shiratsuchi A, Taoka A, Nakanishi Y, Fukumori Y. 2007. Participation of nitric oxide reductase in survival of *Pseudomonas aeruginosa* in LPS-activated macrophages. Biochem Biophys Res Commun. 355(2):587–591.

Kinane DF, Radvar M. 1999. A six-month comparison of three periodontal local antimicrobial therapies in persistent periodontal pockets. J Periodontol. 70(1):1–7.

Lu Y, Slomberg DL, Sun B, Schoenfisch MH. 2013. Shape-and nitric oxide flux-dependent bactericidal activity of nitric oxide–releasing silica nanorods. Small. 9(12):2189–2198.

Lu Y, Sun B, Li C, Schoenfisch MH. 2011. Structurally diverse nitric oxide–releasing poly (propylene imine) dendrimers. Chem Mater. 23:4227–4233.

Papapetropoulos A, García-Cardeña G, Madri JA, Sessa WC. 1997. Nitric oxide production contributes to the angiogenic properties of vascular endothelial growth factor in human endothelial cells. J Clin Invest. 100(12):3131–3139.

Privett BJ, Broadnax AD, Bauman SJ, Riccio DA, Schoenfisch MH. 2012. Examination of bacterial resistance to exogenous nitric oxide. Nitric Oxide. 26(3):169–173.

Radvar M, Pourtaghi N, Kinane DF. 1996. Comparison of 3 periodontal local antibiotic therapies in persistent periodontal pockets. J Periodontol. 67(9):860–865.

Riccio DA, Schoenfisch MH. 2012. Nitric oxide release, part I: macromolecular scaffolds. Chem Soc Rev. 41(10):3731–3741.

Schairer DO, Chouake JS, Nosanchuk JD, Friedman AJ. 2012. The potential of nitric oxide releasing therapies as antimicrobial agents. Virulence. 3(3):271–279.

Shin JH, Metzger SK, Schoenfisch MH. 2007. Synthesis of nitric oxide–releasing silica nanoparticles. J Am Chem Soc. 129(15):4612–4619.

Silva Mendez L, Allaker R, Hardie J, Benjamin N. 1999. Antimicrobial effect of acidified nitrite on cariogenic bacteria. Oral Microbiol Immunol. 14(6):391–392.

Slomberg DL, Lu Y, Broadnax AD, Hunter RA, Carpenter AW, Schoenfisch MH. 2013. Role of size and shape on biofilm eradication for nitric oxide–releasing silica nanoparticles. ACS Appl Mater Interfaces. 5(19):9322–9329.

Stöber W, Fink A, Bohn E. 1968. Controlled growth of monodisperse silica spheres in the micron size range. J Colloid Interface Sci. 26(1):62–69.

Williams RC, Paquette DW, Offenbacher S, Adams DF, Armitage GC, Bray K, Caton J, Cochran DL, Drisko CH, Fiorellini JP. 2001. Treatment of periodontitis by local administration of minocycline microspheres: a controlled trial. J Periodontol. 72(11):1535–1544.

Worley BV, Slomberg DL, Schoenfisch MH. 2014. Nitric oxide–releasing quaternary ammonium-modified poly (amidoamine) dendrimers as dual action antibacterial agents. Bioconjugate Chem. 25(5):918–927.